Drift velocity and temporal phase fluctuations of sliding charge density waves in Rb0.3MoO3

P. Butaud, P. Ségransan, A. Jánossy, C. Berthier

J. Phys. France **51** (1990) 59-89 1er JANVIER **1990**, PAGE 59

Classification
Physics Abstracts
71.45L — 72.15N — 76.60C

Drift velocity and temporal phase fluctuations of sliding charge density waves in $Rb_{0.3}MoO_3$

P. Butaud, P. Ségransan, A. Jánossy (*) and C. Berthier

Laboratoire de Spectrométrie Physique (associé au C.N.R.S.), Université Joseph Fourier, Grenoble 1, B.P. 87, 38402 St Martin d'Hères, France

(*Reçu le 19 septembre 1989, accepté le 20 septembre 1989*)

Résumé. — Nous observons le mouvement de l'onde de densité de charge dépiégée sous l'effet d'un champ électrique par des mesures de transport, de tension de bruit et par une étude RMN, effectuées sur le même monocristal de $Rb_{0,3}MoO_3$. L'observation de bandes latérales dans le spectre RMN en présence du mouvement de l'onde constitue une mesure directe de ν_d, la fréquence locale d'oscillation de la modulation de la charge de l'onde. L'étude de l'amplitude de l'écho de spin permet une mesure résonante de la même quantité ν_d. La comparaison avec les mesures de tension de bruit qui présentent un pic d'intensité à ν_n, confirme nos résultats antérieurs montrant que ν_d et ν_n sont égaux à 10 % près. Les spectres RMN relevés à $E/E_T \approx 20$ (E_T est le champ électrique seuil de dépiégeage) et dans la plage de température 40-60 K sont très bien reproduits par les simulations numériques assimilant la densité spectrale de bruit à la distribution spatiale de la vitesse de l'onde. Nos résultats s'interprètent bien en considérant le cristal comme une collection de domaines. A l'intérieur de chaque domaine la modulation du champ hyperfin reste cohérente pendant environ 25 à 50 périodes. Enfin nous discutons des fluctuations temporelles de la phase de l'onde de densité de charge qui deviennent importantes à haute température et plus spécialement près du champ électrique seuil.

Abstract. — The dynamics of CDW-s depinned by an electric field is investigated by transport, voltage noise and NMR measurements on a $Rb_{0.3}MoO_3$ single crystal. A direct measurement of the bulk winding rate ν_d of the sliding CDW phase is provided by the observation of sidebands in the motionally narrowed NMR spectra and by the oscillations of the spin echo amplitude as a function of the delay time. Comparison with the noise spectra confirms our earlier statement that ν_d is equal to the voltage noise frequency ν_n with an accuracy of 10 %. Experimental NMR spectra at a field of $E/E_T \approx 20$ (E_T is the depinning threshold) in the temperature range of 40 to 60 K have been fitted with high accuracy to lineshapes calculated under the assumption that the noise spectrum is related to the spatial current distribution in a simple way. Most of the experiments can be interpreted by considering the crystal as a collection of domains. In each domain the current is coherent for long times, we found in some cases a temporal coherence of 25-50 oscillation periods of the hyperfine field. We discuss stochastic variations of the CDW phase which become important at high temperatures, especially at fields near threshold.

(*) *Permanent address :* Central Research Institute for Physics, H 1525, Budapest 114, Hungary.

1. Introduction.

Sliding Charge Density Waves (CDW), sometimes called the Fröhlich mode, is a collective excitation of the electron-phonon system of some materials with a quasi one dimensional electronic structure [1]. Its most obvious signature is the appearance of a non-linear current above a threshold applied field. By now there is no doubt that the extra current observed first in $NbSe_3$ [2], and since in a few other systems, is due to the sliding of charge density waves as a whole, the best evidence is the motional narrowing [3] and the appearance of sidebands [4] of the Nuclear Magnetic Resonance (NMR) spectrum under current. A number of questions regarding the Fröhlich mode remain however unsettled. In particular it was realized soon [5] that a constant CDW current is accompanied by a periodic voltage oscillation, but the origin of these oscillations and in particular the role of CDW phase slip lines has not yet been clarified.

The present work is an extension of earlier studies [3b, 4], it deals with electrical transport and ^{87}Rb NMR of a $Rb_{0.3}MoO_3$ crystal in the sliding CDW state. The emphasis is on the temporal variation of the CDW phase. $Rb_{0.3}MoO_3$ is representative in most respect of all sliding CDW systems ; its crystal and CDW structure together with the transport properties have been thoroughly investigated [1]. After a brief survey of the basic quantities measured (Sect. 2) and an account of the experiment techniques (Sect. 3) we deal with the transport properties (Sect. 4). The presentation of NMR data is preceded by a survey of the theory of the NMR lineshapes (Sect. 5), the discussion is limited to the conditions of the experiment. NMR in CDW systems has been reviewed recently in reference [6]. In section 6 free precession and spin echo Fourier Transform (FT) spectra together with spin-spin relaxation time data obtained at various temperatures and applied electric fields are presented. The emphasis is on the measurement of the drift velocity and the random phase fluctuations of the CDW. A more complete description of NMR in sliding CDW systems will be published elsewhere [7]. The drift velocity is measured in a direct resonant way by spin-echo. In the discussion (Sect. 7) we correlate the transport and NMR data obtained on the same crystal. We confirm our earlier assertion that the CDW winding rate equals the frequency of the voltage noise. We separate effects due to temporal fluctuations of the CDW phase from those due to spatial inhomogeneity of the current. At low temperatures temporal random fluctuations of the local field are measurable but not very important. At temperatures above 70 K and for moderate electric fields we arrive at the unexpected conclusion that the phase fluctuates with large amplitude even in regions of the sample where, due to imperfections, the average current is zero.

2. The sliding CDW state.

A one dimensional uniform metallic chain is unstable against a periodic distortion with wavevector $2\pi/\lambda = 2k_F$ where k_F is the Fermi momentum. Weak interactions between chains lead to a three dimensionally ordered distorted state below the Peierls transition temperature T_P where the charge density wave has the form :

$$\rho = \rho_0 + \rho_1 \cos(\mathbf{q} \cdot \mathbf{R} + \varphi) \tag{2.1}$$

here ρ_0 is the uniform density, ρ_1 the CDW amplitude, in the mean field theory proportional to the magnitude of the order parameter. The component of the wavevector along the chain $q_y = 2k_F$ is determined by the band filling ; q_x, q_z depend on weak interactions between the chains. The CDW phase φ in absence of an applied electric field may be determined by the lattice, by impurities or other imperfections, or by the boundaries of the crystal. Interactions

with the lattice fixes φ if the system is commensurate i.e. if $q_y = q_0 = \frac{n}{m}\frac{2\pi}{b}$ where b is the lattice constant along the uniform chain, n and m are small integers. For band fillings leading to nearly commensurate wavevectors the CDW is expected to consist of commensurate regions interrupted by discommensurations where φ is varying. There are two extreme cases for this « nearly commensurate » phase where discommensurations are : i) an array of 2D phase slip narrow walls separated by $\frac{1}{m}\frac{2\pi}{|q-q_0|}$ or ii) broad walls, a weak modulation of the phase φ with period $\frac{2\pi}{|q-q_0|}$.

If the lattice potential is not strong and the system is incommensurate the CDW is represented to a good approximation by a plane wave with a slow variation of the phase determined by impurities or other imperfections. In the theory of Fukuyama and Lee [8] and Lee and Rice [9] the impurity pinning is called strong if φ has the same value at all impurity sites or, alternatively, weak if the phase at any point in the crystal depends on the collective action of a large number of impurities. In high purity $K_{0.3}MoO_3$ the phase may be coherent over more than 1 μm along the chain and nearly 1 μm transverse to the chain [10]. In cases where neither the lattice nor impurities are important the main source of pinning may be macroscopic defects (e.g. inclusions) or the boundaries of the crystal.

A small electric field polarizes the CDW. Above a threshold value E_T the electric energy gained by displacing the CDW by a wavelength exceeds the energy gained by adjusting the phase to the pinning potential and the CDW becomes depinned and slides with a drift velocity :

$$v_d = \frac{\lambda}{2\pi}\frac{d\varphi}{dt}, \quad \text{where} \quad \lambda = \frac{2\pi}{q_y} \tag{2.2}$$

v_d may be measured by the current j_{CDW} associated to the Fröhlich mode

$$j_{CDW} = \rho_c v_d \tag{2.3}$$

where ρ_c is the condensed electron density which at tempeatures much below T_P equals the uniform electron density $\rho_0 = \frac{2e}{\lambda}n$, n is the density of conducting chains per unit area perpendicular to their direction times the band degeneracy.

Alternatively, the phase winding rate

$$\nu_d = \frac{1}{2\pi}\frac{d\varphi}{dt} \tag{2.4}$$

may be measured directly by NMR by observing the temporal variation of the hyperfine field at sites on or nearby the chain. In the static case the NMR spectrum is inhomogeneously broadened by the spatial variation of the hyperfine field which follows the variation of the CDW. The drifting CDW modulates periodically the hyperfine field and the corresponding change in the NMR spectrum allows a direct measurement of ν_d. We note that one could measure ν_d by the energy change of neutron diffraction superlattice reflexions (Doppler shift) [11]. This method would be equivalent to the NMR method, it also measures ν_d.

If the CDW is an ideal plane wave driven by a constant force ν_d is constant and equal to the periodicity of the local hyperfine field variation. If, however, the CDW is inhomogeneous or the forces acting on it vary with time ν_d will also fluctuate. For example a sliding CDW interacting with a single impurity encounters a potential varying periodically in time. Periodic and random fluctuations have an entirely different effect on the NMR spectra.

In all sliding CDW systems, even for a constant external driving field, a fluctuation is superimposed on the CDW drift. The average frequency of this current oscillation is proportional to the average current. Several mechanisms have been proposed to explain this phenomenon. In the impurity model [8] it is assumed that the boundaries of the crystal are unimportant but rather the system may be thought of being divided into domains with dimensions equal to the corresponding coherence lengths. In the sliding state in each domain the overall pinning force of the impurities varies periodically with the difference between the equilibrium and instantaneous phases.

In the vortex model [9, 12] the current oscillations are due to a periodic generation and annihilation of CDW phase dislocation lines at the interface of pinned and unpinned regions. Both models predict that the fundamental current oscillation frequency ν_n equals the phase winding rate.

$$\nu_n = \nu_d \,. \tag{2.5}$$

Bardeen [13] suggested a theory where $\nu_n = 2\,\nu_d$ and until recently [4] experiments measuring ν_d by the nonlinear current could not provide an unambiguous answer [14]. As we show, a measurement of the local field variation proves (2.5) with good accuracy.

In this paper we show that in addition to the periodic fluctuation of j_{CDW} there is a temperature dependent random fluctuation. In principle, random fluctuations broaden the frequency spectrum measured by a noise spectrum analyser. However the broadening of the noise spectrum peak of a single domain with a homogeneous current is difficult to resolve from an inhomogeneous broadening due to a spatial distribution of the current of an imperfect crystal. By NMR the spatial inhomogeneity of ν_d is distinguished from local random temporal fluctuations of the phase.

3. Experimental.

All new measurements reported in this paper were performed on the same single crystal $Rb_{0.3}MoO_3$ (sample ≠ 2) grown by electrolysis from a melt of MoO_3 and Rb_2MoO_4 by Marcus [15]. It was cut by a wire saw into an approximately rectangular shape ; the length along the crystallographic axis b was 3.60 mm, the cross-section of the ends perpendicular to b was 0.45 mm^2. The NMR coil, had a cross-section only slightly larger than the crystal and was about as long. After being placed in the NMR coil the ends of the crystal were polished, copper plated and contacted with silver paint to thin gold wires. Judging from the current voltage (*I-V*) characteristics and the voltage noise spectra, the crystal quality was somewhat better than those used in previous studies [4].

I-V characteristics and voltage noise spectra were recorded *in situ* in the NMR coil. Usually the current to the sample was continuous except for measurements at 75 and 87 K where the NMR spectra were taken by a pulsed technique to avoid heating. *I-V* characteristics were measured by a quasi four point method. Although this method does not eliminate contact resistance we believe this has no influence on the data. At room temperature the resistance of the sample together with contacts was less that 0.1 Ω.

The noise spectra were taken with an HP 8568 A spectrum analyser connected to an HP 9836 computer. A baseline taken with field below threshold was subtracted and then the noise intensity $V^2(\nu)/\mathrm{BW}$ calculated (here V is the amplitude of the voltage fluctuations and BW the instrumental bandwidth). The spectra were distorted by 50 cycles interference at frequencies below 1 kHz. A small variation of the gain of the preamplifier and transmission line was noted, this affects somewhat the intensity data for large frequency spans but is unimportant in the determination of the average frequencies.

The free induction decay (and in some cases the spin echo) of the (− 1/2, + 1/2) transition of site (2) ^{87}Rb (in the notation of Ref. [16]) was recorded at $\nu_0 = 80.132$ MHz by a BRUKER CXP-100 spectrometer. The external magnetic field $H_0 = 5.175$ T was applied along the c^* axis (perpendicular to the *a-b* plane). The amplitude of the rotating field H_1 was 70 G, and the dead time of the receiver was less than 6 μs. Signals were averaged and Fourier transformed by a NICOLET LAS 12/70 signal analyser. To improve the S/N ratio a systematic phase alternation of the $\frac{\pi}{2}$ pulses $\frac{\pi}{2}\Big|_x - \frac{\pi}{2}\Big|_y$ was applied combined with sign inversion of the acquired data. Also a reasonable offset was chosen between ν_0 and the center of the spectrum to avoid the formation of a spurious FFT image in the frequency range of interest. Final phase adjustments were made by an HP 9836 computer.

4. Measurement of transport properties.

4.1 CURRENT-VOLTAGE CHARACTERISTICS. — The threshold voltage V_T for the onset of non-linear conduction was measured between 43 and 78 K (Fig. 1). At all temperatures the threshold is well defined although at lower temperatures a small uncertainty arises from the difference between increasing and decreasing field measurements. Between 43 and 60 K E_T increases only by a few percent, at higher T the increase is much faster. These results are in agreement with those reported in the literature [1].

A typical conductivity *versus* electric field characteristics is shown in figure 2. The non-linear CDW current is determined by subtracting the normal current extrapolated from the low field value :

$$I_{CDW} = I - V/R_n .$$

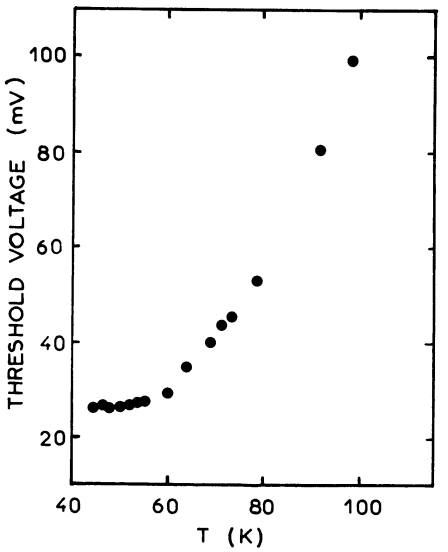

Fig. 1.

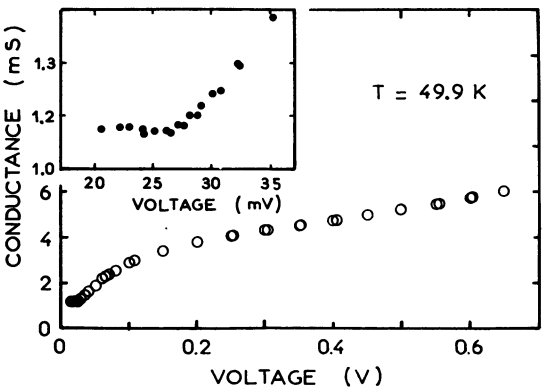

Fig. 2.

Fig. 1. — Variation of the threshold voltage (sample # 2) *versus* temperature T. It is measured *in situ in the NMR coil.*

Fig. 2. — Typical conductivity *versus* electric field (sample # 2).

This extrapolation may not be entirely valid for two reasons : i) R_n, the normal resistance depends on electric history and may be somewhat different in the depinned state ; ii) the onset of the CDW current may be accompanied by a normal current backflow [17]. We assume in the analysis of data that these effects are not important.

The normal conductivity has an activated behaviour as a function of temperature with activation energy $E_a^n = 490$ K (Fig. 3). This value is the same as found in other crystals indicating that the crystal is pure enough to be an intrinsic semiconductor above 40 K. The CDW conductivity I_{CDW}/V is also activated, the energy depends somewhat on the field, at $V = 200$ mV $E_a^{CDW} = 743$ K while at $V = 600$ mV $E_a^{CDW} = 837$ K (Fig. 3). Although these energies were determined in a relatively narrow temperature range (43 to 55 K) they still convincingly show that E_a^{CDW} is substantially larger than E_a^n.

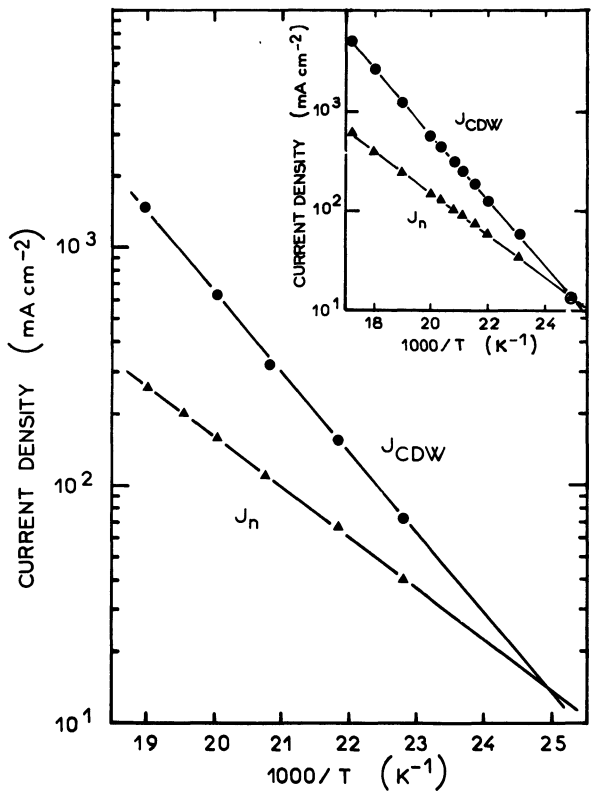

Fig. 3. — CDW (circles) and normal (triangles) current densities as a function of the inverse temperature. The data in the inset (sample ≠ 1) were taken at a field of 1.5 V/cm, and those of the main figure (sample ≠ 2) at 1.67 V/cm. The normal current is extrapolated from low field data.

The CDW is not depinned in the entire sample at V_T, and due to the inhomogeneity of the current density j_{CDW}, the *I-V* characteristics do not give the correct dependence of j_{CDW} on E. Nevertheless, the similarity of the characteristics at different temperatures suggests that the distribution of j_{CDW}/I_{CDW} within the crystal does not change significantly with temperature, at least for large E/E_T ratio.

4.2 VOLTAGE NOISE SPECTRA. — Applying a constant current through the sample above threshold induces a voltage $V(t)$ fluctuating in time. In $NbSe_3$, in some cases where the CDW current may be homogeneous within the sample $V(t)$ is nearly periodic and the frequency spectrum $V^2(\nu)$ of the fluctuations of $V^2(t)$ consists of a narrow line with harmonics. In the $Rb_{0.3}MoO_3$ sample investigated the voltage fluctuation spectra are complex mainly due to an inhomogeneity of the CDW current over the cross-section.

Voltage spectra were recorded at temperatures between 40 and 87 K at various bias fields. The form of the spectra depends strongly on the applied voltage but for a given voltage, spectra taken at different temperatures may be scaled on to each other.

Figure 4 shows noise intensity spectra at a fixed temperature (53.5 K) at various applied fields V (35.4, 70, 250, 600 mV). For V just above threshold a few narrow peaks appear, at twice threshold a large number of peaks are resolved, at even higher fields narrow lines are no more resolved. At $V = 600$ mV the spectrum consists of a broad peak with some structure and a tail increasing sharply at low frequencies.

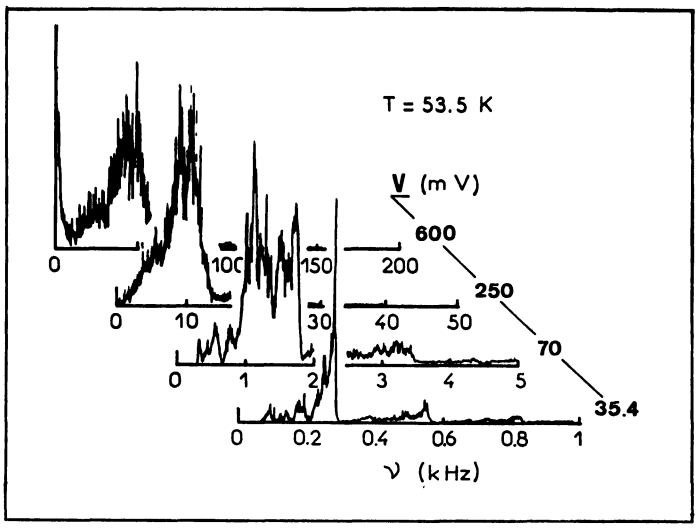

Fig. 4. — Noise power spectra taken at $T = 53.5$ K in sample # 2. The shape of these spectra radically changes with applied field.

Spectra at a fixed field ($V = 600$ mV) at 42, 50 et 55 K demonstrate the scaling with temperature (Fig. 5).

Although the average frequencies $\bar{\nu} = \dfrac{\int \nu V^2(\nu)\,d\nu}{\int V^2(\nu)\,d\nu}$ differ by a factor of 70 the noise intensity distributions are quite similar. At low temperatures the low frequency tail could not be resolved at $V = 600$ mV, increasing the field to higher values it appears, however, with large intensity.

For understanding the origin of noise the variation of its time averaged amplitude $\langle |V(t)|^2 \rangle^{1/2}$ with field and temperature is of special interest [12]. Accurate measurements

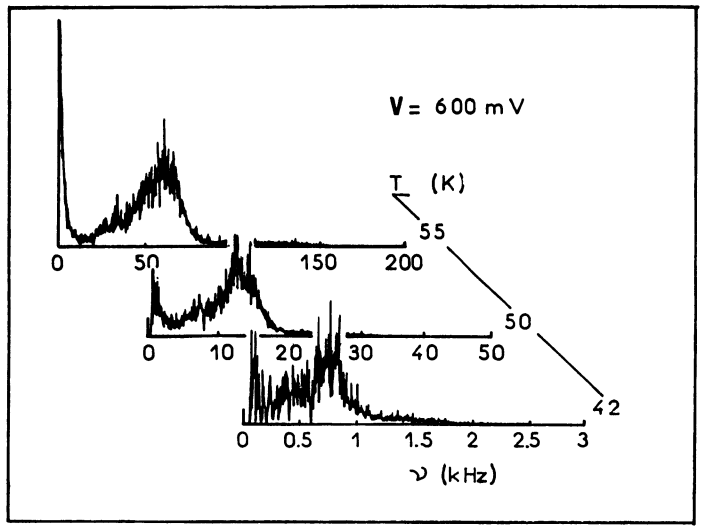

Fig. 5. — Noise power spectra taken at $E = 1.67$ V/cm in sample # 2. The first harmonic component has been subtracted from the raw data. Note the similarity of the spectra despite a change of a factor 60 in the frequency scale. The voltage power $|V(\nu_n)|^2$ changes inversely to the mean frequency so that the total intensity remains constant.

are difficult to perform since the transmission line connecting the sample to the spectrum analyzer is somewhat frequency dependent. Also, the change of the current distribution with field renders the interpretation uncertain. Nevertheless, it may be concluded from figure 6 that the noise amplitude does not vary strongly with field and temperature.

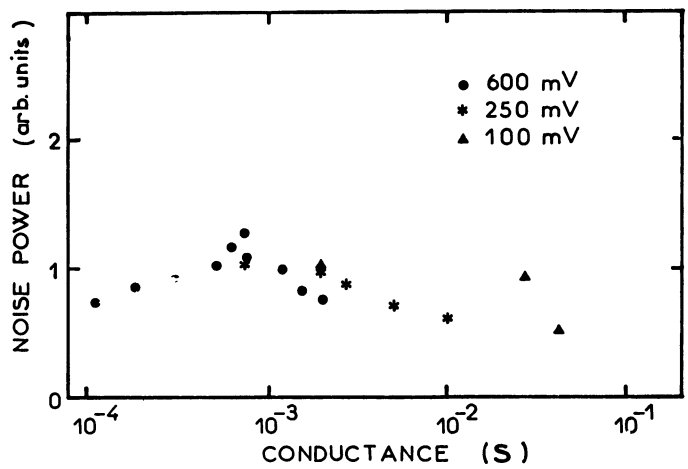

Fig. 6. — Noise power $|V(t)|^2$ taken at different values of E and T. Despite the variation of the conductivity by three orders of magnitude, $|V(t)|^2$ stays constant within a factor of 2.

5. Survey of NMR in $Rb_{0.3}MoO_3$.

Before presenting the experimental results a brief description of NMR and spin echo spectra in quasi one dimensional CDW systems is given. The discussion is limited to aspects relevant to our experiments on ^{87}Rb in $Rb_{0.3}MoO_3$.

5.1 NMR SPECTRUM, STATIC CDW. — The interaction of the nucleus at site $\mathbf{R}_i$ with its surroundings is given by

$$H(\mathbf{R}_i) = H_Z + H_Q + H_{hf} + H_d \,. \tag{5.1.1}$$

Under our experimental conditions the quadrupolar, magnetic hyperfine and dipolar interactions (second to fourth terms respectively) are a perturbation of the Zeeman term H_Z. The Rb nucleus is not included in the conducting chain and the magnetic hyperfine term is negligible compared to the quadrupolar coupling even above the Peierls transition. The dipolar term determines the homogeneous part of the linewidth in both the metallic phase and below the Peierls transition without an applied electric field. The quadrupolar term shifts the Zeeman levels and splits the threefold degeneracy of the transition frequencies of the $I = \frac{3}{2}$ ^{87}Rb nuclei. We consider in the following the $-1/2 \rightarrow +1/2$ central transition only.

The quadrupolar interaction is proportional to the electric field gradient tensor $V_{\alpha\beta}$

$$H_Q = \frac{eQ}{6\,I(2\,I-1)} \sum_{\alpha\beta} V_{\alpha\beta} \left(\frac{3}{2} (I_\alpha I_\beta + I_\beta I_\alpha) - \delta_{\alpha\beta} I^2 \right) .$$

The parameters $\nu_Q = e^2 qQ/2\,h$ with $eq = |V_{ZZ}|$ and $\eta = (V_{XX} - V_{YY})/V_{ZZ}$ together with the directions of the principle axis X, Y, Z were determined for the Rb sites in the metallic phase by Douglass *et al.* [18].

The resonance frequency is shifted in second order of ν_Q/ν_0 from the Larmor frequency $\nu_0 = \gamma H_0$ (with H_0 the applied static magnetic field and γ the gyromagnetic ratio) [19] :

$$\Delta\nu = -\frac{\nu_Q^2 (I(I+1) - 3/4)}{6\,\nu_0} f(\eta, \theta, \phi) \tag{5.1.2}$$

where θ and ϕ are the polar and azimuthal angles of the external field with respect to the principal axis and $f(\eta, \theta, \phi)$ can be found in reference [19].

Above the Peierls transition in the geometry of the experiment $\theta = \phi = \frac{\pi}{2}$, from reference [8] $\eta = 0.5$ and thus

$$\Delta\nu^0 \approx \frac{\nu_Q^2}{8\,\nu_0} . \tag{5.1.3}$$

We decompose $\Delta\nu$ into two parts : $\Delta\nu = \Delta\nu^0 + \delta\nu$ where $\Delta\nu^0$ arises from the undistorted lattice while $\delta\nu$ represents the frequency shift due to the CDW.

The EFG originates from distant ions and delocalized electrons and from electrons on the site of interest in the case where wave functions are hybridized with the conduction band. The effect of distant charges is amplified by the Sternheimer antishielding factor [20].

For on site electrons the antishielding factor is close to 1 but the contribution to the EFG

$$q = \sum_k \left\langle \psi_k \left| \frac{P_z(\cos\theta)}{|\mathbf{r} - \mathbf{R}_i|^3} \right| \psi_k \right\rangle \tag{5.1.4}$$

may still be large because ψ_k is not small at small values of $|\mathbf{r} - \mathbf{R}_i|$.

The contribution to the EFG due to the overlap of delocalized electrons of the Mo-O clusters with the Rb sites is not necessarily negligible compared to the ionic contribution ; in the case of Na_xWO_3 for example the overlap of d-band conduction electrons with the Na wavefunction gives rise to well observable Knight shift and Korringa relaxation of the ^{23}Na nuclei [21].

In the metallic state there are two Rb sites Rb(1) and Rb(2), with symmetries $2/m$ and m respectively, which have different resonance frequencies. In this work Rb(2) was investigated. Below the Peierls transition a CDW appears coupled to a periodic lattice distortion (PLD) and the position of site j is displaced from the average position R_j by :

$$\Delta \mathbf{R}_j = \mathbf{\Delta}_1 \cos (qR_j) + \mathbf{\Delta}_2 \sin (qR_j) \tag{5.1.5}$$

in the plane wave approximation. The modulation vectors $\mathbf{\Delta}_{1,2}$ were determined for $K_{0.3}MoO_3$ (a compound very similar in all respect to $Rb_{0.3}MoO_3$) by Shuttle and de Boer [22].

The displacements of various sites have similar temperature dependences and are proportional to the order parameter of the CDW given by equation (2.1). At $T = 100$ K the order of magnitude of $|\mathbf{\Delta}_{1,2}|$ is 10^{-2} Å [22]. The wavevector $\mathbf{q}$ is found to be $(0, q_b, 1/2)$ in reciprocal lattice units with q_b close to 3/4 below $T = 100$ K [23].

The CDW and PLD modulates the EFG tensor, ν_Q, η and the directions of the principal axes vary periodically between well defined values for sites along the crystallographic direction **b**. A first principles calculation of the modulation of $\delta\nu$ as a function of position is unfeasible. A point charge model taking into account the displacement of distant ions given by (5.1.5) would neglect the covalent nature of the Mo-O bonds and also the variation of the on site contribution (5.1.4).

The resonant frequency varies periodically with wavelength $\lambda = \dfrac{2\pi}{q}$ along the b axis and to second order in the order parameter the modulation of $\Delta\nu$ is :

$$\delta\nu (R_i) = \nu_1 \cos (qR_i + \varphi_1) + \nu_2 \cos^2 (qR_i + \varphi_2) \tag{5.1.6}$$

where ν_1 and ν_2 are proportional to the order parameter and to its square respectively. ν_1, ν_2, φ_1 and φ_2 are determined by the CDW induced change of all parameters of the EFG. A variation in the largest component of the EFG tensor results in a change of ν_Q^0 by $\delta\nu_Q(R_i)$:

$$\Delta\nu^0 + \delta\nu = [\nu_Q^0 + \delta\nu_Q(R_i)]^2/8\,\nu_0 = \Delta\nu^0\left(1 + \frac{2\,\delta\nu_Q(R_i)}{\nu_Q^0} + \left(\frac{\delta\nu_Q(R_i)}{\nu_Q^0}\right)^2\right) \tag{5.1.7}$$

with $\Delta\nu^0$ is given by equation (5.1.3).

The term quadratic in $\delta\nu_Q$ is negligible and the shift $\delta\nu = (2\,\Delta\nu^0/\nu_Q^0)\,\delta\nu_Q(R_i)$ is linear in the displacement despite that the EFG perturbes the energies in second order only.

For a long wavelength $\dfrac{2\pi}{q} \gg b$ a local approximation may be valid and φ_1 $(= \varphi_2)$ may be equal to the phase of the local displacement [24]. In special cases where the site has a particular symmetry ν_1 is zero. This is not the case in our study. We have checked experimentally that for the Rb(2) site of interest the dominant term is linear in the order parameter ($\nu_1 \gg \nu_2$), since the splitting of the lineshape below T_P evolves symmetrically with respect to the position of the line in the undistorted phase [24].

From (5.1.6) the resonance lineshape resulting from the distribution of the EFG is readily calculated [24].

If ν_2 is negligible and as long as q is incommensurate :

$$g(\nu) = \frac{\text{const.}}{\left(1 - \left(\frac{\nu}{\nu_1}\right)^2\right)^{1/2}} \qquad |\nu| < \nu_1 \tag{5.1.8}$$

$$g(\nu) = 0 \qquad |\nu| > \nu_1$$

where ν is measured from the unperturbed resonance frequency $\nu_0 + \Delta\nu^0$.

For nearly commensurate wavevectors large deviations from the plane wave PLD given by (5.1.6) are expected due to the interaction of the CDW with the periodic lattice potential. In the so called « nearly commensurate » phase, observed in some two dimensional systems, the CDW is composed of commensurate regions interrupted by discommensurations in which the phase of the CDW varies rapidly [25]. In $Rb_{0.3}MoO_3$ below 100 K the deviation from the commensurate wavevector $\mathbf{q}_0 = (0, 3/4, 1/2)$ is very small [26] and it was suggested [27] that an incommensurate commensurate (IC-C) transition takes place. Such a commensurate phase has not been found by NMR [6, 28, 29] although indications of a C phase in part of the crystals below 50 K has been found by ESR [30]. In a commensurate system there are only a finite number of inequivalent sites and the NMR spectrum consists of a small number of lines instead of the distribution (5.1.8). There are 32 Rb(2) and 16 Rb(1) sites in the expected commensurate unit but due to the symmetry of the PLD for both sites only 8 have different resonance frequencies for an arbitrarily oriented magnetic field. A careful study of the Rb(1) lineshape at $T = 77$ K has shown that if there are any discommensurations in the system their width is comparable to their separation [28].

Figure 7a shows a fit of (5.1.8) to a experimental spectrum of Rb(2) at 77 K. The values of ν_1 and ν_2 are 4.9 kHz and 0.7 kHz respectively. Figure 7b shows the best fit obtained by varying the width α^{-1} of the walls of a discommensuration lattice

$$\varphi(R) = \sum_{n=-\infty}^{+\infty} \left(\text{Arctg}\left(\exp - 2\,\alpha\left[R - \left(n + \frac{1}{2}\ell\right)\right]\right)\right) \tag{5.1.9}$$

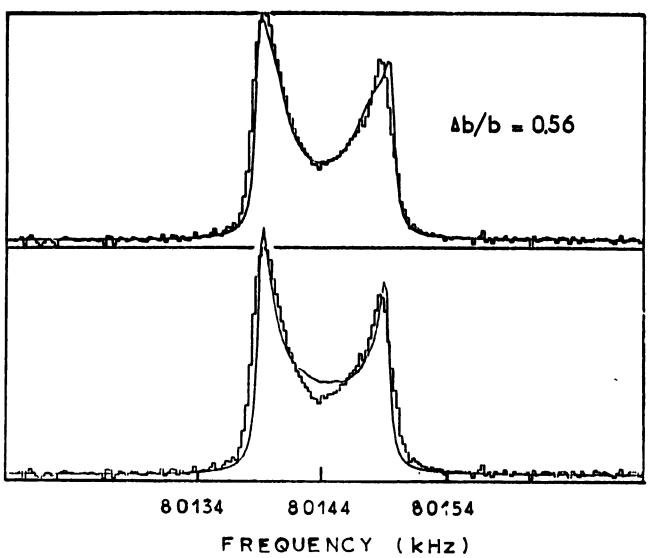

Fig. 7. — Comparison of computer simulations to the experimental lineshape of ^{87}Rb in $Rb_{0.3}MoO_3$. Bottom : plane wave limit, top : multisoliton lattice.

where, ℓ, the distance between two walls, was chosen arbitrarily equal to 1 000 interatomic distances [28].

5.2 NMR SPECTRA FOR A SLIDING CDW. — In the following we use an adiabatic approximation and assume that for a depinned CDW the resonance frequency at site R is determined by the instantaneous phase $\varphi(R, t)$ of the CDW.

Thus in (5.1.6) $\delta\nu(R)$ is replaced by

$$\delta\nu(R, t) = \nu_1 \cos(qR + \varphi_1(R, t)) + \nu_2 \cos^2(qR + \varphi_2(R, t)) . \tag{5.2.1}$$

In the simplest case the phase velocity is constant in time and uniform in space and

$$\delta\nu(R, t) = \nu_1 \cos(q(R - v_d t) + \varphi_1) + \nu_2 \cos^2(q(R - v_d t) + \varphi_2) \tag{5.2.2}$$

with

$$qv_d = \frac{d\varphi}{dt} = 2\pi\nu_d .$$

The simple uniformly sliding plane wave approximation may not be entirely correct in describing the CDW motion. As suggested by Lee and Rice [9] the current may be transported by a series of loop dislocations. Far from the dislocation center the change of the amplitude of the order parameter may be neglected and the variation of φ is non uniform but still periodic. The situation is similar to the motion of a discommensuration lattice. Although the dislocation loops or discommensurations may be widely spaced, the periodicity of the oscillations of the EFG at a given site is the same as for a plane wave CDW provided the same (average) current is flowing. The phase winding rate in general for an array of discommensurations with finite width moving with velocity v_{dc} is (supposing the system to be fourth order commensurate)

$$\frac{d\varphi(R)}{dt} = v_{dc}\,\delta q + \sum_{n=1}^{\infty} \alpha_n \cos(4nv_{dc}\,\delta q t - q_0 R) \tag{5.2.3}$$

where α_n depends on the form and width of the discommensuration and $\delta q = q - q_0$ is the deviation of q from the commensurate value.

The exact solution of the sine Gordon equation, in the limit of broad discommensurations can be shown to be $\varphi(R) = \alpha\,\delta q R + \beta \cos 4\,\delta q R$ [28].

For discommensurations of large wall widths or far from phase slip dislocation lines the α_n-s are small and the main term is the time averaged phase winding rate :

$$\overline{\frac{d\varphi}{dt}} = v_{dc}\,\delta q = 2\pi\nu_d . \tag{5.2.4}$$

For equal current, the phase winding rate of a sliding plane wave and that of a discommensuration lattice are equal. Near dislocation lines, if dislocations are narrow, the harmonics in (5.2.3) may be important in the calculation of the NMR spectra. In this case the assumption of a constant amplitude of the order parameter is, however, unjustified. The periodic generation and anihilation of phase dislocations at the boundaries or the uneven motion due to the impurity pinning potential also give rise to harmonics like those in (5.2.3) but, except for very small currents, the amplitude of the current oscillations is small compared to the average CDW current and do not influence much the NMR spectrum.

In the following we discuss the NMR spectra for a plane wave CDW. We first consider a drift velocity which is constant in time. The effect of non-periodic fluctuations of φ is deferred to section 5.4.

We first return to (5.2.2) where $d\varphi/dt = 2\pi\nu_d$ is uniform in space and time. The correlation function of the transverse magnetization $\langle I_x(t)\, I_x(0)\rangle$ is :

$$G(t) = e^{-i2\pi(\nu_0+\Delta\nu_0)t}\langle I_x(t)\, I_x(0)\rangle = \sum_{R_i} \exp\left(i2\pi \int_0^t \delta\nu(R_i, t')\, dt'\right). \quad (5.2.5)$$

Neglecting the quadratic term and using the formula

$$e^{ix\sin(\varphi)} = \sum_{n=-\infty}^{\infty} J_n(x)\, e^{in\varphi} \quad (5.2.6)$$

and assuming an incommensurate CDW for which

$$\sum_{R_i} e^{i(n-n')qR_i} = \delta_{nn'} \quad (5.2.7)$$

we find

$$G(t) = \sum_{n-\infty}^{+\infty} \left[J_n\left(\frac{\nu_1}{\nu_d}\right)\right]^2 e^{i2\pi n\nu_d t} = J_0\left(\frac{2\nu_1}{\nu_d}\sin(\pi\nu_d t)\right). \quad (5.2.8)$$

The NMR line shape is the Fourier transform of $G(t)$

$$\tilde{G}(\nu) = \sum_{n-\infty}^{+\infty} \left[J_n\left(\frac{\nu_1}{\nu_d}\right)\right]^2 \delta(\nu - n\nu_d). \quad (5.2.9)$$

These expressions were first derived, in a slighty different way by Kogoj *et al.* [31].

It is natural that in (5.2.8) the correlation function $G(t)$ is periodic in time since we have considered up to now a deterministic periodic local hyperfine field modulation. The NMR spectrum (5.2.9), is composed of a central line ($n = 0$) and sidebands at $\nu = \pm n\nu_d$. The central line is analogous to the usual motional narrowing (except that it has zero width). The sidebands are analogous to those observed in High Resolution NMR in solids where the sample is spining at a magic angle to average out the dipolar fields. Just as the position of the sidebands is a direct measure of the angular velocity of the rotor in Magic Angle Spinning, the position of the sidebands in $\tilde{G}(\nu)$ for a uniformly sliding CDW measures the CDW phase velocity $v_d = \nu_d \frac{2\pi}{q}$. The amplitude of the sidebands decreases rapidly with increasing v_d since $J_n(x) \propto x^n$ for small x (Fig. 8a), for $\nu_d > \nu_1$ nearly all the intensity is in the central line.

The effect of the quadratic term in (5.2.6) on the lineshape is found by a straightforward calculation :

$$\tilde{G}(\nu) = \delta\left(\nu - \frac{\nu_2}{2}\right) * \sum_{n=-\infty}^{+\infty} A_n\left(\frac{\nu_1}{\nu_d}, \frac{\nu_2}{\nu_d}\right) \delta(\nu - n\nu_d). \quad (5.2.10)$$

The exact expression for A_n is given elsewhere [7, 28]. For $\nu_d/\nu_1 > 2$, 90 % of the intensity is included in the central line and the only effect of the quadratic term is a shift by $\nu_2/2$ to higher frequencies.

In the actual crystals the current is not homogeneous in space and instead of a single drift velocity we have to consider a distribution $P(v_d)$. We have in mind a crystal with a large number of domains, in each domain the current is homogeneous and slides with a velocity

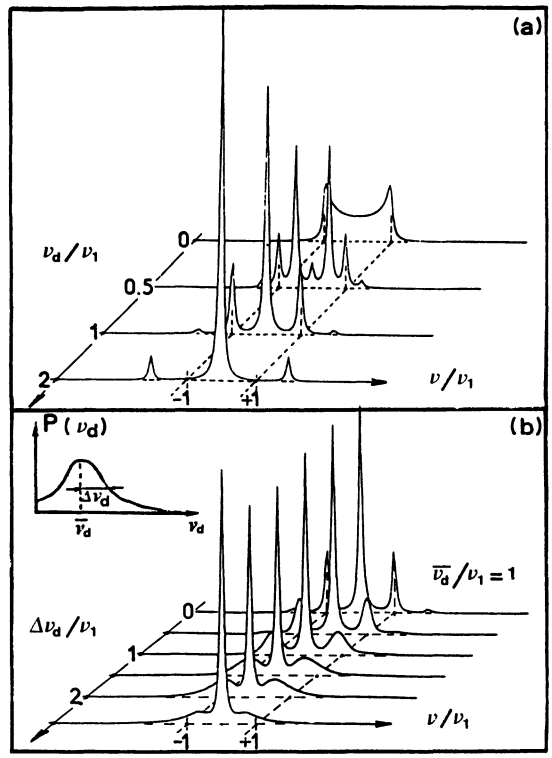

Fig. 8. — (a) Theoretical NMR lineshape in presence of a CDW sliding with a uniform velocity $v = \nu_d \lambda$. The local hyperfine shift is $\nu(R) = \nu_1 \cos(qR + 2\pi\nu_d t + \phi_0)$. (b) Variation of the NMR lineshape as a function of the width of a Gaussian velocity distribution $P(\nu_d) = \exp - \left\{ \frac{(\nu_d - \bar{\nu}_d)^2}{2(\Delta\nu_d)^2} \right\}$ at a fixed value $\bar{\nu}_d = \nu_1$.

v_d. The form of the central line $n = 0$ is not affected by a velocity distribution since it is independent of v_d in contrast to sidebands which are broadened (Fig. 8b) and we find :

$$\tilde{G}(\nu) = \delta\left(\nu - \frac{\nu_2}{2}\right) * \left[\tilde{G}_S(\nu) \int J_0^2\left(\frac{\nu_1}{\nu_d}\right) P(\nu_d)\, d\nu_d + \right.$$

$$\left. + \sum_{n \neq 0} P\left(\frac{\nu}{n}\right) J_n^2\left(\frac{n\nu_1}{\nu}\right) * \tilde{G}_S(\nu)\right]. \qquad (5.2.11)$$

The lineshape of both the central and sideband components are broadened by the dipolar interaction between neighboring nuclei, characterized by the spin-spin relaxation rate T_2^{-1}. Perturbation of delocalized electrons, strains around defects and mosaicity are also of importance, the linewidth above the Peierls transition is inhomogeneous and much larger than expected from the dipolar interaction alone. The dipolar contribution to the linewidth is somewhat decreased by a static CDW, neighbouring Rb nuclei at sites i and j become « unlike » in this case since their corresponding EFG-s are different, i.e. the spin flip-flop terms $I_i^+ I_j^-$ become ineffective in inducing dipolar transitions. A sufficiently rapid motion of

the CDW leads to an effective hyperfine field which is the same for all nuclei and causes the flip-flop term to reappear. The value of T_2 is then expected to be similar to that measured just above the Peierls transition, a situation where inhomogeneous broadening due to the screening of charged impurities have already developed.

5.3 SPIN-ECHO IN PRESENCE OF A SLIDING CDW. — Spin-echo is the traditional way to measure the homogeneous spin-spin correlation time T_2. It enables the distinction between homogeneous and inhomogeneous contributions to the NMR linewidth. The sliding of the CDW dramatically changes the echo and this offers a method to measure in a direct way the drift velocity v_d.

In the static case the form of the echo centered at 2τ (where τ is the delay between the $\pi/2$ and π r.f. pulses) is given in the plane wave approximation (neglecting ν_2) by :

$$G_e(t) = J_0(2\pi\nu_1(t-2\tau))\, e^{-t/T_2} \tag{5.3.1}$$

and the echo amplitude has the usual exponential form. The onset of the CDW motion modifies the amplitude [7, 28] :

$$I(2\tau) = J_0\left[\frac{4\nu_1}{\nu_d}\sin^2(\pi\nu_d\tau)\right] e^{-2\tau/T_2}. \tag{5.3.2}$$

The echo amplitude oscillates as a function of τ with a period $2\pi/\nu_d$. These oscillations are more pronounced for low drift velocities, if $\nu_d < 1.6\,\nu_1$ the amplitude becomes even negative in some intervals of τ. The effect is somewhat smeared by a distribution of ν_d :

$$I(2\tau) = \int J_0\left(\frac{4\nu_1}{\nu_d}\sin^2(\pi\nu_d\tau)\right) P(\nu_d)\, d\nu_d \tag{5.3.3}$$

but as we show in section 6.2 the effect remains well observable.

For large values of t (i.e. $\pi\nu_d\tau$ large), (5.3.3) leads to a constant value $\int_0^\infty a_0(\nu_d)\,P(\nu_d)\,d\nu_d$ where $a_0(\nu_d)$ is the zero-frequency Fourier component of the periodic function $J_0\left(\frac{4\nu_1}{\nu_d}\sin^2(\pi\nu_d t)\right)$. This constant is of course multiplied by e^{-t/T_2} where T_2 is the spin-spin relaxation time which includes the spin-spin dipolar interaction and the effect of the stochastic fluctuations of the CDW velocity.

Further information on the CDW motion is gained from an analysis of the shape of the echo for $t \geqslant 2\tau$ [7, 28] :

$$G_e(2\tau + t) = \sum_{n=-\infty}^{+\infty} J_n(w)\, J_n\left(\frac{\nu_1}{\nu_d}\right) e^{-in(\chi - 2\pi\nu_d\tau)}\, e^{-i2\pi n\nu_d t}\, e^{-\frac{t+2\tau}{T_2}} \tag{5.3.4}$$

where

$$w = (\nu_1/\nu_d)(5 - 4\cos 2\pi\nu_d\tau)^{1/2} \tag{5.3.5a}$$

$$\sin\chi = \frac{\sin 2\pi\nu_d\tau}{(5 - 4\cos 2\pi\nu_d\tau)^{1/2}}. \tag{5.3.5b}$$

As we see the Fourier transform of $G_e(2\tau + t)$ is similar to (5.2.9) in the sense that it is composed of a central line and sidebands at $\pm n\nu_d$, but the relative intensities of these

components differ from those obtained from the Fourier transform of the free induction decay and depend on τ. Under special conditions the intensity of the central line may even be zero, e.g. if $\nu_1/\nu_d = 0.8$ and $\nu_d \tau = 1/2$; the intensity of the sidebands is increased by 40 %.

5.4 STOCHASTIC FLUCTUATIONS OF THE VELOCITY ; SPIN-SPIN RELAXATION TIME. — Up to now we have considered a constant or a periodically modulated CDW velocity. We have seen that this leads to a periodic correlation function for the transverse magnetization $G(t)$ and in this case the damping is due to the nuclear magnetic dipole-dipole interaction characterized by the relaxation time T_{2d}. In the presence of a static CDW we found $T_{2d} = 4.6$ ms in $Rb_{0.3}MoO_3$; it is slightly shorter if the CDW is sliding with a fast constant velocity as mentioned in section 5.2.

Random fluctuations of the CDW phase may drastically increase the damping of $G(t)$ and have a much more pronounced effect than the slight change of the dipolar interaction due to the CDW motion. In general we would like to describe the effect of a time and position dependent phase $\varphi(R, t)$ with a periodic and a non periodic component. We first neglect the periodic variation of φ and assume that it is varied in time by a Markovian process. For example, we consider a nucleus in a Fukuyama Lee Rice domain which, due to a random fluctuation of the average phase, experiences a hyperfine shift $\nu(t_1)$, $\nu(t_2)$, ... $\nu(t_i)$ at times t_1, t_2, ..., t_i..., with $|\nu(t_i)| < \nu_1$ and a jumping rate of τ_c^{-1} to jump from one frequency to another. These conditions correspond to the usual stochastic process of motional narrowing of a hyperfine structure [32]. For $\tau_c^{-1} \ll 2\pi\nu_1$ the hyperfine broadening of the NMR line remains intact but the spin-spin relaxation rate T_2 increases proportionally to τ_c. For $\tau_c^{-1} \sim 2\pi\nu_1$ the hyperfine structure of the spectrum is destroyed and T_2 reaches its maximum of $(2\pi\nu_1)^{-1}$ which would be a very short value of the order of 30 μs in our particular case. For $\tau_c^{-1} \gg 2\pi\nu_1$ the spectrum consists of a single line centered at the first moment of the hyperfine distribution and T_2 becomes proportional to $(2\pi\nu_1)^2 \tau_c$.

Clearly the above description is not adequate for describing the experimental NMR lineshape under current since the motional narrowing due to the phase change with constant rate is neglected. Indeed the observed T_2 does not follow the above description.

In the following we outline the behaviour when both the random and constant phase variations are taken into account. Let us define the random function :

$$\delta W(R, t) = 2\pi\nu_1 \left(\int_0^t \cos\left(qR + \varphi(R, t')\right) dt' - \int_0^t \cos\left(qR + 2\pi\nu_d t'\right) dt' + \varphi_0 \right) \quad (5.4.1)$$

and the periodic function :

$$W(R, t) = 2\pi\nu_1 \int_0^t \cos\left(qR + 2\pi\nu_d t' + \varphi_0\right) dt' . \quad (5.4.2)$$

The correlation function of the transverse magnetization is given by

$$G(t) = \sum_{R_i} \left\langle e^{iW(R_i, t) + \delta W(R_i, t)} \right\rangle = \sum_{R_i} e^{iW(R_i, t)} \left\langle e^{i\delta W(R_i, t)} \right\rangle \quad (5.4.3)$$

where the bracket denotes a statistical average over various physical realizations of the random function $\varphi(R, t)$.

A general calculation of $G(t)$ is complex, we confine the discussion to some limiting cases. At high velocities we may take $e^{iW(R, t)} = 1$. We assume the amplitude of the random phase

fluctuations is small and that its variation may be decoupled from the spatial dependence, i.e. $\varphi(R, t) = \varphi(t) = \varphi_0 + \delta\varphi(t) + 2\pi\nu_d t$. Supposing $|\delta\varphi(t)| \ll \frac{\pi}{2}$ for all t, the function

$$\delta W(t) = 4\pi\nu_1 \int_0^t \frac{\sin \delta\varphi(t')}{2} \sin\left(qR + \frac{2\pi\nu_d t' + \varphi(t') + \varphi_0}{2}\right) dt'$$

may be approximated by $2\pi\nu_1 \int_0^t \delta\varphi(t')\, dt'$ which overestimates the effect of fluctuations. Assuming a Gaussian stationary process, we find for times $t \gg \tau_c$ the correlation time of the phase, the usual result [32] :

$$\langle e^{iW(t)} \rangle = \exp(-(2\pi\nu_1)^2 \overline{\delta\varphi}^2 \tau_c t) \tag{5.4.4}$$

while for $t \ll \tau_c$:

$$\langle e^{iW(t)} \rangle = \exp(-(2\pi\nu_1)^2 \overline{\delta\varphi}^2 t^2). \tag{5.4.5}$$

We emphasize that the above results are obtained by employing severe approximations on the motion and in particular we assumed that the drift velocity is fast. The calculation is limited to electric fields $E \gg E_T$ where fluctuations due to the pinning are small compared to the constant winding of the phase. An approximation which is more adequate to fields close to threshold is the following :

We do not consider the amplitude of the fluctuations to be small. Thus we assume the motion to be coherent for short times ($\varphi(t) = 2\pi\nu_d t$) but with a probability Γ per unit time that an event changes the motion drastically. We assume $\delta W(R, t)$ changes so much that nuclei at the position where the event happens contribute no more to the echo. Thus the number of nuclei refocused at time 2τ (for a pulse sequence $\frac{\pi}{2}$ — τ — π) is $N(2\tau) = N(0)\, e^{-2\Gamma\tau}$ and the amplitude of the echo is

$$J_0\left(\frac{4\nu_1}{\nu_d} \sin^2(\pi\nu_d \tau)\right) e^{-2\Gamma\tau}. \tag{5.4.6}$$

More generally, in expression (5.2.11) $G_S(\nu)$ has to be replaced by $G_D(\nu)$, a function taking into account broadening from the phase fluctuations as well as the static imperfections and the dipolar relaxation rate.

Finally let us recall the case treated by Kogoj *et al.* [31] where the CDW is depinned thermally and $\nu_d = 0$. Here also, one distinguishes small and large amplitude fluctuations. For $\delta\varphi(R, t) \ll \frac{\pi}{2}$ the static lineshape is observed, while for $\delta\varphi(R, t) \gg \frac{\pi}{2}$ and for short t the motional narrowing is complete. Approximating $\delta\varphi(R, t)$ by :

$$\delta\varphi(R, t) = B \sin(\omega_0 t) \sin\left(\frac{\pi R}{\ell_0}\right)$$

where ℓ_0 is the average distance between pinning centers, ω_0 is of the order of the lowest phason frequency and B is the root mean square thermal fluctuation amplitude, one finds a reduction of the splitting of the edge divergences of the static spectrum as B increases from zero. Further increasing B a central peak appears and finally the whole intensity merges into the central line, the width of which decreases with increasing B. Contrary to a coherent

motion where sidebands appear, the spectrum in this picture is strictly confined to the frequency interval $|\delta\nu| < \nu_1$.

6. NMR results.

In a previous set of experiments [4] (on sample $\neq 1$) we studied the variation of the NMR lineshape in the temperature range of 40-60 K at a fixed applied field $E = 15\ E_T$. The new results (on sample $\neq 2$) are in agreement with the previous ones. Figure 9 displays the variation of the NMR lineshape with temperature of the previous crystal. At 40 K, although the current voltage characteristics and the noise spectrum show that the CDW is depinned, the CDW velocity is too small to change the lineshape. As j_{CDW} increases with increasing the temperature the edges of the spectrum broaden and diminish and a peak emerges at the center frequency of the static spectrum. On further increase of j_{CDW} (by increasing T) the central peak becomes the most prominent part of the spectrum. At the intermediate current of $j_{CDW} = 0.405$ A/cm^2 additional steps arise at the sides of the spectrum outside the range of the static line.

In presenting the new NMR results on the sample characterised in sections 3 and 4 we focus on three aspects :

i) the variation with temperature and field of the fraction f_s for which the CDW remains static ;

ii) the variation with temperature and field of the spin-spin relaxation time due to the stochastic fluctuation of the CDW phase ;

iii) a more detailed account is given of the sidebands in the free precession spectrum. Their origin is confirmed by a spin-echo experiment under the same applied current.

6.1 STATIC FRACTION OF THE CDW AND THE SPIN-SPIN RELAXATION. — Figure 10 shows f_s, the fraction of the crystal in which the CDW is pinned, at various electric fields and temperatures. f_s is obtained by a fit of the free precession lineshapes $\tilde{G}(\nu)$ to the expression

$$\tilde{G}_S(\nu) = f_s\, \tilde{G}_S(\nu) + (1 - f_s)\, \tilde{G}_D\left(\nu - \frac{\nu_2}{2}\right)$$

where $\tilde{G}_S$ is deduced from a fit of the lineshape with no applied current to the theoretical expression and $\tilde{G}_D(\nu)$ is a Gaussian as shown in the insert. f_s depends on both field (normalized to E_T) and temperature. At 64 K a clear increase of the static fraction is observed as the field is decreased towards E_T. On the other hand for E/E_T between 2.5 to 3 the tendency of a decrease of the static fraction with an increase of temperature above 64 K is well observed.

The spin-spin relaxation time, T_2, data measured at various temperatures and fields are plotted in figure 11. At high electric fields ($E/E_T > 3$) the decay is exponential while at lower fields ($E/E_T < 3$) it is composed of two exponentials. An example is shown in figure 12. The fast decay T_{2F} corresponds to nuclei in domains where the CDW is sliding (or at least fluctuating) while the slow decay T_{2L} corresponds to domains with a static CDW. In figure 11 T_{2F} is shown. T_{2L} is equal to 4.2 ms at all temperatures i.e. it equals the relaxation rate in absence of any current applied to the sample.

The static fraction f_s' may be deduced from the T_2 measurements by fitting the amplitude of the echo to the expression :

$$G_e(t) = f_s' \exp\left(-\frac{t}{T_{2L}}\right) + (1 - f_s') \exp\left(-\frac{t}{T_{2F}}\right).$$

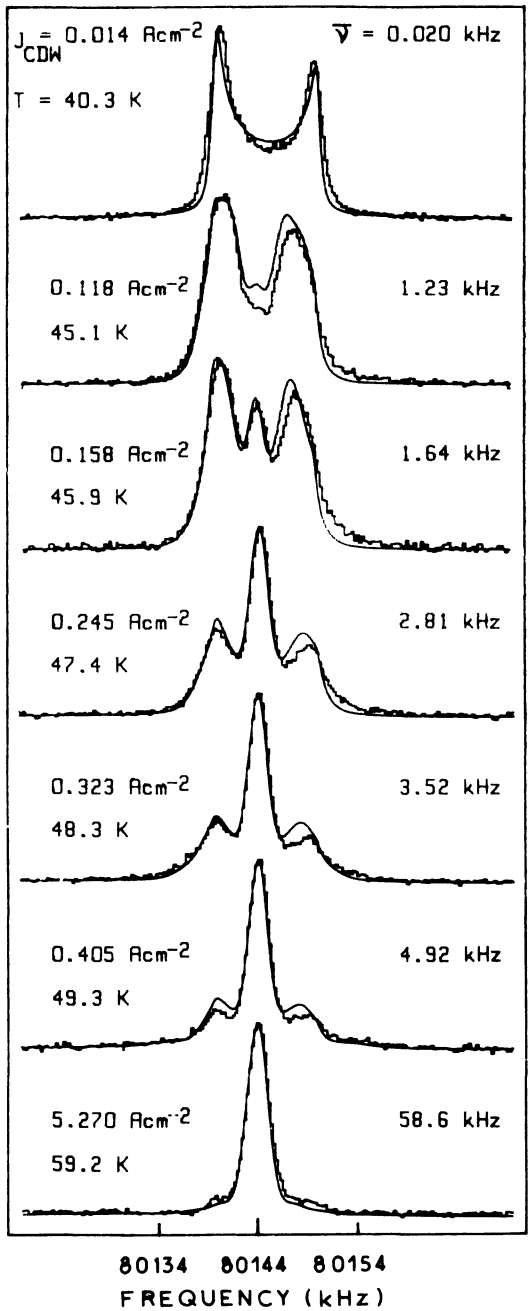

Fig. 9. — Variation of the NMR lineshape and computer-fitted curves as functions of the CDW current j_{CDW} for sample # 1. The field is fixed at $E = 1.5$ V/cm ($\sim 15\ E_T$) and the temperature is varied to change j_{CDW} for sample # 1. For the computer simulated spectra the relative CDW velocity distribution is determined from the experimental noise spectrum at 59.2 K. For each simulated spectrum only one parameter, the average local-field oscillation frequency $\bar{\nu}_d$, was fitted.

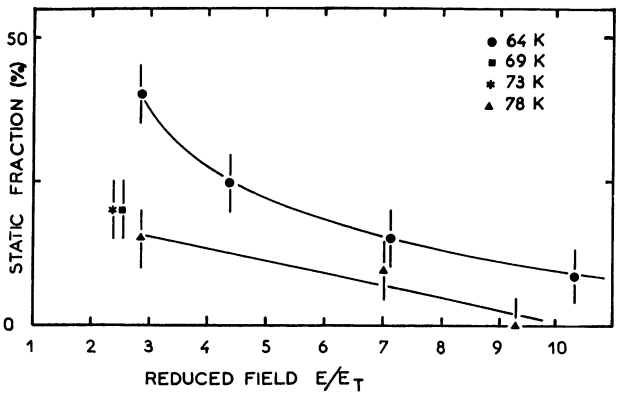

Fig. 10.

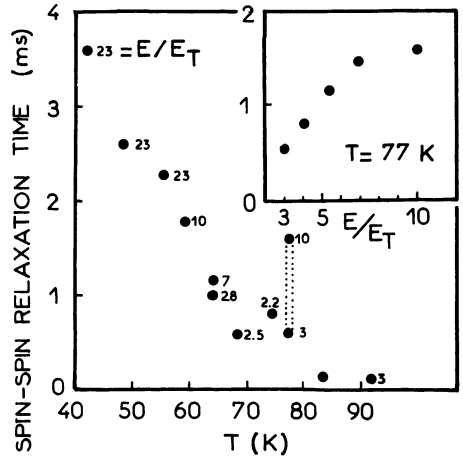

Fig. 11.

Fig. 10. — Variation of the static fraction f_s (in which the CDW is pinned) as a function of E/E_T at various temperatures.

Fig. 11. — Variation of the dynamic spin spin lattice relaxation time T_{2F} *versus* temperature. The number on the right of each point is the ratio E/E_T.

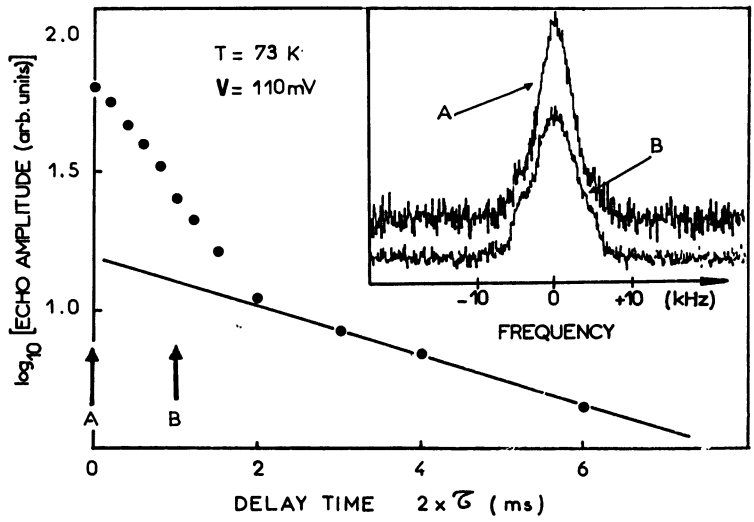

Fig. 12. — Variation of the amplitude of the spin-echo as a function of the delay time τ at $T = 73$ K and $V = 110$ mV ($\approx 3\,V_T$). The longest time constant for the decay corresponds to nuclei in regions of the crystal were the CDW is pinned, whereas the short one corresponds to nuclei in regions were the CDW is sliding. The inset shows the Fourier Transforms of the half of the spin-echo for two different delay times ($\tau = 0$ and 500 μs, indicated by the arrows A and B. The weight of the static contribution increases with τ.

The values of f_s' and f_s deduced from the lineshape of the free precession are in reasonably good agreement.

The Fourier transform of the echo lineshape at 73 K and delay time $2\tau = 1$ ms shows that at longer times the static component becomes dominant if the CDW is not depinned in the full sample. This explains the failure of Douglass *et al.* [33] to observe any change in the echo lineshape in $Rb_{0.3}MoO_3$ with a voltage well above threshold. They used an echo delay time of $2\tau = 1$ ms for which the contribution of the dynamic central line vanishes (due to non periodic fluctuations of the phase) and they observed only a reduction of the intensity of the static line.

In the following when referring to T_2 under current we implicitly mean that the static fraction of $G(t)$ has been subtracted. The most obvious feature of the relaxation time results is the rapid decrease of T_2 with increasing temperature. The data must be considered with some caution since they are not taken at the same values of $E/E_T = \alpha$. The inset shows the variation of T_2 as a function of α at 77 K where the dependence is strong. At 63 K a much less pronounced field dependence is observed.

6.2 COHERENCE EFFECTS. — In this section we review experiments at temperatures below 50 K where sidebands and the oscillation of the echo amplitude, predicted by equations (5.2.9) and (5.3.2) respectively, were observed. Figure 13 shows for a small temperature range the variation of the lineshape at a fixed electric field ($V = 600$ mV $\approx 24\ V_T$). Arrows indicate the position of the peak in the voltage noise spectra at the same temperatures. The $p = \pm 1$ sidebands situated at about the frequency of the peak of the noise spectra are well observable ; they shift to higher frequencies as the average current is increased.

In the present work the sidebands are better resolved than in the previous study [4]. The spectrum has, however, a component resembling the static line (due to parts of the crystal

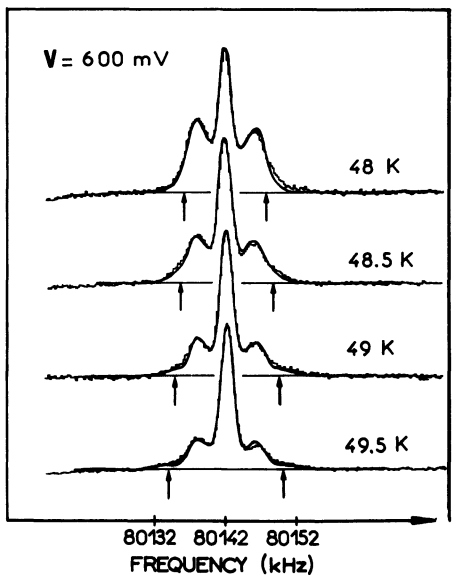

Fig. 13. — NMR spectra giving evidence for the NMR sidebands $n = \pm 1$ in sample # 2. The simulated spectra were computed using 7.5 from the experimental noise spectra taken at the same electric field (1.67 V/cm) and temperature. The arrows indicate the position of the peak in the experimental noise spectra (see Fig. 5).

with slowly moving CDW) which hinders the observation of sidebands for $\nu_d/\nu_1 \approx 1$ where their intensity is large. Due to these wings around ν_1 the optimum condition for observing the sidebands is $\nu_d/\nu_1 \approx 1.5$ where, however their intensity is only 10 % of the total.

The wings of the spectra at about $\pm \nu_1$ only resemble a static line but in fact they arise from regions of the crystal where the CDW is sliding, even if slowly. These regions are also the source of the low frequency upturn in the noise frequency spectrum. A comparison of the wings with the static line is shown in figure 14. Due to the movement and the phase fluctuations the wings are broadened and their maxima are shifted towards the center line.

A clear proof for the motion of the CDW in practically the whole sample is given by the Fourier Transform (FT) of the spin echo at a delay time $2\tau = 250$ μs (Fig. 15). As explained in section 5.3 the intensity of the sidebands observed in the FT of the echo depends on ν_1/ν_d and τ. By appropriately choosing τ the contribution to the echo FT from the low frequency part of the distribution of ν_d is strongly reduced while the central line is barely affected. The amplitude of the echo FT of static regions does not depend on τ for such small values and since at some frequencies within $\pm \nu_1$ the echo FT is about zero we conclude that for $E = 600$ mV, $T = 49$ K the static fraction f_s is also about zero.

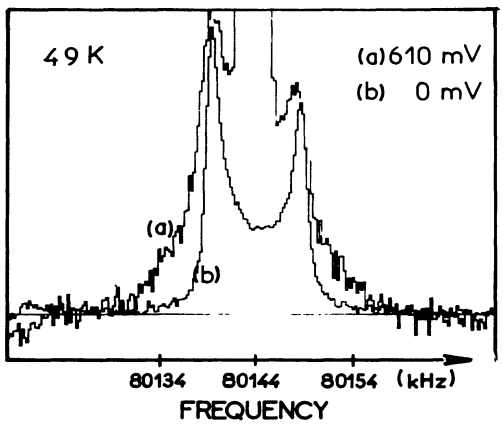

Fig. 14.

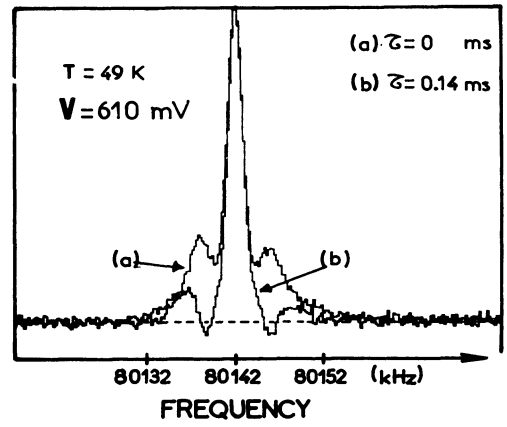

Fig. 15.

Fig. 14. — Comparison of ^{87}Rb spectra taken at $V = 600$ mV (a) and $V = 0$ mV (b) at $T = 49$ K. Besides the sidebands, spectrum (a) shows two peaks at the same position as those of spectrum b. However, for (a) they are broader due to the dynamics of the slowly sliding CDW in those parts of the crystal which contribute to the low frequency tail of the noise spectra.

Fig. 15. — NMR spectra taken at $T = 49$ K and $V = 610$ mV by Fourier Transform of a) the free induction decay, b) half of the spin echo ($\tau = \mu$s). This delay time has been chosen to cancel the contribution of the nuclei belonging to parts of the crystal in which the CDW is slowly sliding. This cancellation is a consequence of the coherence of the CDW motion, and could not occur if the CDW were merely static.

The time coherence of the CDW phase is observed in a direct and resonant way by the variation of the amplitude of the echo $I(2\tau)$ as a function of τ, shown for $T = 49$ K in figure 16. A deep minimum in $I(2\tau)$ is observed at $\tau = 80$ μs. This delay time corresponds well to the condition $2\pi\nu_p\tau = \pi/2$ where ν_p is the peak frequency of the

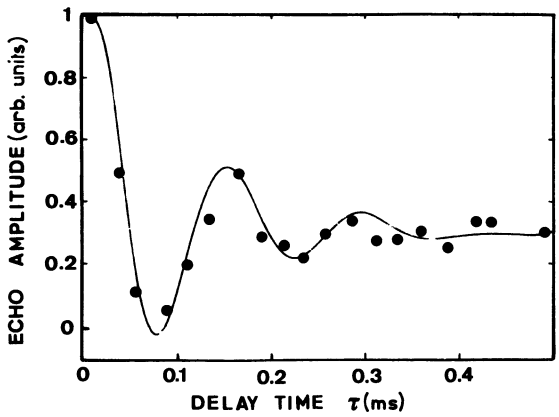

Fig. 16. — Experimental variation of the amplitude of the spin echo as a function of the delay time τ in $Rb_{0.3}MoO_3$ at $E/E_T \sim 20$ and 49 K. The solid curve is the convolution of the theorical dependence $J_0(4\,\nu_1/\nu_d \sin^2(\pi\nu_d\,\tau))$ with the experimental distribution $P(\nu_d)$ obtained from the noise spectra.

voltage noise spectrum at the same temperature and field. A damped periodic behaviour is observed with a period of ν_p^{-1} and a damping constant related to the width of the noise peak. At larger values of $2\,\tau$ the oscillations are completely damped and $I(2\,\tau)$ decreases exponentially with a constant time T_2 resulting from the dipolar spin-spin interaction and stochastic fluctuations of the CDW phase.

We stress that the oscillations of $I(2\,\tau)$ are mainly determined by the peak of the noise spectrum. As confirmed by computer simulations [7], the low frequency part of the noise spectra i.e. the slowly moving regions, do not affect much the oscillation period ν_p^{-1} of $I(2\,\tau)$.

A similar experiment at 43 K and 600 mV was also conducted. At this temperature the free induction NMR spectrum is only slightly modified by the motion of the CDW. Although the oscillations in $I(2\,\tau)$ are more complicated than at 49 K they are in complete agreement with the theory. The comparison of $I(2\,\tau)$ with the noise spectrum shows clearly the equivalence of ν_d and ν_n.

7. Discussion.

7.1 EQUIVALENCE OF THE PHASE WINDING RATE AND VOLTAGE NOISE FREQUENCY. — To understand the origin of voltage noise one should first compare its frequency to the phase winding rate. In other words we ask whether the voltage oscillates with the same frequency as the atoms in the chain. A compilation of data has been made by Monceau [14] but the answer was not conclusive. While earlier works were based on a measurement of the current density, in this work we measured the phase winding rate by NMR.

We defer for the moment the discussion of the main assumption that the distribution of the drift velocity is proportional to the voltage noise intensity :

$$P(\nu_d) = f(\nu_n) \tag{7.1a}$$

with

$$\nu_d = \beta\,\nu_n \tag{7.1b}$$

$\beta = 1$ is expected from the impurity and vortex models. In our previous work (on sample $\neq 1$), which is confirmed by the new data on sample $\neq 2$, we fitted β for several spectra with various average noise frequencies $\bar{\nu}_n$ taken between $T = 40$ and 59 K and found $\beta = 1$ fits well while $\beta = 2$ is incompatible with the data.

The present analysis focuses on measurements in a narrow temperature range $T = 48$ to 49.5 K and a large external electric field ($V = 610$ mV), over 20 times the smallest threshold ($V_T = 28$ mV) in the sample.

We calculate the NMR lineshape from (5.2.9) and (7.1) assuming $\beta = 1$. The amplitude ν_1 (and ν_2) are found from the static spectrum, these are proportional to the CDW order parameter amplitude (and its square) and are temperature independent in the range of interest. The dipolar and other small broadenings effects are taken into account by a Gaussian

$$\tilde{G}_S(\nu) = e^{-\frac{(\nu - \nu_0)^2}{2\sigma^2}} \tag{7.2}$$

where σ was measured from a fit to the central line of the measured dynamic spectra. At low temperatures σ is nearly temperature independent, random CDW fluctuations add a negligible contribution.

In the theory of the noise one expects the fundamental noise frequency to be equal to the phase winding rate thus to obtain $f(\nu)$ we have subtracted the first harmonic from the measured spectrum $f_m(\nu)$:

$$f(\nu) = f_m(\nu) - \alpha f_m(2\nu)\,. \tag{7.3}$$

We find $\alpha = 0.1$ by assuming that at twice the frequency of the peak of f_m the fundamental is zero.

A further assumption on $P(\nu)$ has to be made for very low frequencies $\nu < \nu_{co}$ as below $\nu_{co} = 1$ kHz $f(\nu)$ could not usually be measured.

In our previous work on sample $\neq 1$ we used the experimental noise spectra at 59.2 K (after removal of the first harmonic) as a master curve for the phase winding rate distribution $P(\nu/\bar{\nu}_d)$. The NMR spectra were calculated according to (5.2.10) adjusting $\bar{\nu}_d$ to obtain the best agreement with experimental data (Fig. 9). For very low velocities corresponding to $\nu_d = v/\lambda < 0.17$ kHz, the dynamic lineshape given by (5.2.9) was replaced by the static asymmetric one. The reason was that the dynamic histograms calculated for these low frequencies are indistinguishable from the static ones calculated for $\nu_2 = 0$. As can be seen the agreement is fairly good, the main features of the spectra are quite well reproduced for average values of ν_d ranging from 0.020 kHz to 58.6 kHz. We found the ratio $\bar{\nu}_d/j_{CDW} = 11 \pm 1$ kHz A.cm^{-2} by averaging over fits to NMR spectra at seven temperatures. This value is in close agreement with the value of 12.5 kHz/A cm^{-2} expected for the conduction electron density of $Rb_{0.3}MoO_3$.

In the following we discuss new data on sample $\neq 2$ demonstrating that $\nu_n = \nu_d$. At $V = 600$ mV the static fraction of the sample where the phase is constant in time is negligible as shown by the measurement of the spin echo (see Sect. 6.2) ; this means $P(0)$ is finite. The simplest approximation is

$$\begin{aligned} P(\nu) &= f(\nu) \qquad \nu > \nu_{co} \\ P(\nu) &= f(\nu_{co}) \quad \nu < \nu_{co}\,. \end{aligned} \tag{7.4}$$

The calculated NMR spectra at $T = 49$ K shown in figure 17 are in good agreement with the measured ones. We stress that for these spectra there is no fitting parameter apart from σ

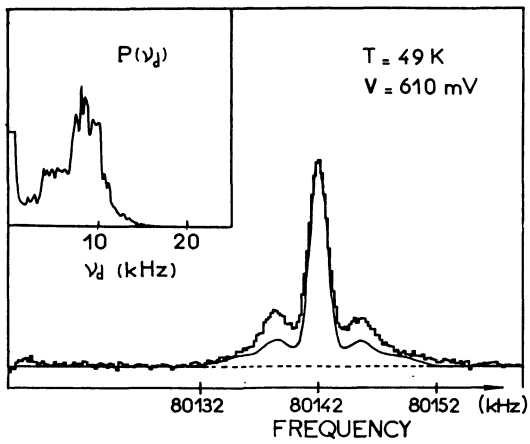

Fig. 17. — NMR spectrum at 49 K and its computer simulation using (7.4) from the experimental noise spectrum shown in the inset. The sibedands $n = \pm 1$ are fairly well reproduced, bu the difference in the quality of the fit with that of figure 13 results from the leveling of the amplitude of the low frequency tail of the noise spectrum.

which is known approximatively from the high temperature data. The best proof of the equivalence of $\nu_d = \nu_n$ is that the sidebands are correctly reproduced. An assumption of $\nu_n = 2\,\nu_d$ would lead to calculated sidebands displaced from the center by half the observed ones and they would be masked by the central part of the line.

The agreement between calculated and experimental spectra is perfect if an appropriate low frequency distribution of $P(\nu)$ is chosen :

$$\begin{aligned} P(\nu) &= f(\nu) && \nu > \nu_{co} \\ P(\nu) &= P(0) + [f(\nu_{co}) - P(0)]\,\nu/\nu_{co} && \nu < \nu_{co}\,. \end{aligned} \tag{7.5}$$

Here $P(0)$ is a fitted parameter. This extrapolation is justified by the large intensity of $f(\nu)$ for low ν found at higher temperatures where for the same electric field $f(\nu)$ is shifted to higher frequencies.

Similarly to the previous lineshape calculations [4, 7, 28], the dynamic histogram is replaced by the static one for $\nu < 0.17$ kHz, but in the new calculation histograms are convoluted with the same broadening function for both low and high frequencies since we know from the spin echo measurement that there is no part in the crystal were the phase of the CDW is time independent. Any attempt to consider the low frequency part as purely static (i.e. folded with the same broadening function as used in the static case) led to a worse agreement between the experimental and calculated lineshapes. The best fit for the fraction of the crystal where the noise frequency is less than 1 kHz is

$$\int_0^{\nu_{co}} P(\nu)\,\mathrm{d}\nu = 0.3\text{-}0.5\,, \tag{7.6}$$

somewhat depending on temperature.

The equivalence $\nu_d = \nu_n$ is unambiguously shown by the spin echo amplitude $I(2\,\tau)$ which for a single domain oscillates with a period $1/\nu_d$. For a peaked velocity distribution these oscillations are readily observed. In figure 16 we plot the dependence of the spin echo

amplitude on delay time calculated from (5.3.2) using the same distribution $P(\nu)$ from (7.5) as for the NMR. The calculated and measured $I(2\tau)$ curves agree very well. An assumption of $\nu_n = 2\nu_d$ would clearly be incompatible with the measurement. We note that the calculated oscillation period of $I(2\tau)$ does not depend on the specific assumption made on the low frequency distribution of $P(\nu)$.

In the above analysis we have assumed that the voltage noise intensities of the domains are simply additive. The approximation (7.1a) is exact for incoherent oscillators in series. In fact the sample is better described by a set of parallel oscillating domains with CDW conductivities σ^i_{CDW} varying from domain to domain. In this model the external average voltage is the same for all domains and the current distribution is due to a variation of threshold fields. The « intrinsic » noise amplitude of the i-th domain $\Delta V_0(\nu_i)$ is reduced by the conductivity of the others

$$\Delta V(\nu_i) = \Delta(\nu_i)(\sigma^i_{CDW}/\sigma)(A_i/A) \tag{7.7}$$

where A_i/A is the cross-section relative to the total and σ is the average conductivity including the normal contribution. The measured spectrum $f(\nu)$ is proportional to $|\Delta V_0(\nu_i)|^2$ averaged over the bandwidths of the frequency fluctuations and the spectrum analyzer. Since σ_{CDW} increases with increasing CDW current the measured voltage noise distribution $f(\nu)$ has a larger weight at larger frequencies than the current distribution $P(\nu)$. The assumption (7.1a) is better justified at large external fields where $\sigma_{CDW}(E)$ tends to level off (Fig. 2).

7.2 RATIO OF THE VOLTAGE NOISE FREQUENCY TO CDW CURRENT DENSITY, ν_n/j. — The measured ratio of $\bar{\nu}_n/j$ normalized to the theoretical value as a function of the normalized field E/E_T is given in figure 18. Here $\bar{\nu}_n = \int_0^\infty \nu f(\nu)\,d\nu$; $f(\nu)$ is defined by (7.3) and

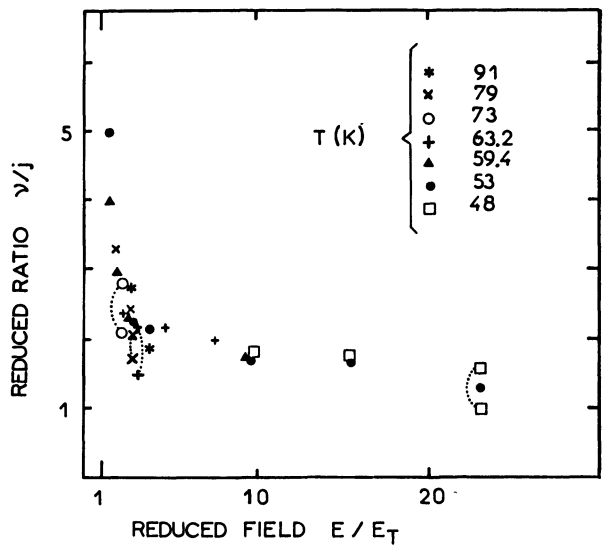

Fig. 18. — $\bar{\nu}_n/j_{CDW}$ (normalized to 12.5 kHz/A cm^{-2}) obtained from voltage noise spectra at various values of E/E_T and temperatures. In some cases the static fraction (i.e. the volume of undepinned regions in the crystal) was determined by NMR and data could be corrected for the static fraction.

$\bar{j}_{CDW} = I_{CDW}/A$ is the current density defined in section 4.1. For $1 < E/E_T < 3$ it decreases steeply with increasing field while for higher values it slowly approaches unity. In the preceding paragraph we demonstrated that $\nu_n = \nu_d$. Since in the temperature range of the experiments the order parameter is practically unity any deviation from the relation $j_{CDW} = \lambda \rho_c \nu_n$ must come from incertitudes in the measured values of j_{CDW} and ν_n. Just above threshold the CDW current flows in a small portion of the sample only and the neglection of regions with $\nu < \nu_{co}$ in $f(\nu)$ leads to large errors in ν_n. This explains the upturn of $\bar{\nu}_n/j$ curve for E/E_T approaching 1.

The NMR experiment provides an unambiguous way to determine the fraction f_s of the sample in which there is no or very little temporal variation of the phase. f_s determined from the free precession lineshape is given in figure 10. At higher fields ($V > 250$ mV) and low temperatures ($T \leqslant 60$ K) the replacement of the frequency distribution $f(\nu)$ by $P(\nu)$ suggested by the NMR analysis improves significantly the agreement between experimental and theoretical values of $\bar{\nu}_n/\bar{j}_{CDW}$ (Fig. 18). At the highest field, 610 mV, where the analysis is the most reliable we found after replacing $f(\nu)$ by $P(\nu)$ $\bar{\nu}_n/j_{CDW} = 12.5$ kHz, a remarkably good agreement with theory.

However, contrary to what is expected from the noise spectra, we find that the static fraction measured by NMR depends not only on field but also on temperature. It decreases with increasing temperature for a fixed field. Thus at high temperatures f_s measured by NMR is much less than expected from the ν_n/j_{CDW} ratio. At 79 K and $E/E_T = 2.3$ according to the noise spectra there is no CDW current in 50 % of the sample while by NMR $f_s \approx$ 15 %. Thus we believe that at high temperatures large amplitude phase fluctuations occur in regions where there is no or negligible CDW current. This may be an indication for an electric field assisted thermal depinning. Thermal depinning of the phase (« floating phase ») has been observed in incommensurately modulated dielectrics [24].

A quite different model for the variation of the static fraction with field and temperature has been suggested by Tucker *et al.* [34]. It was assumed that the current flows in a rather particular way : it advances by 2 π jumps due to the appearance and disappearance of CDW phase slips. They claim that as long as the average drift frequency ν_d is smaller than the dielectric relaxation frequency ν_0 the 2 π jumps of the phase are not significantly smeared and the NMR spectrum is not narrowed by the motion. To support this view they consider the results of Ross *et al.* [3a] on $NbSe_3$ where the condition $\nu_1 < \nu_d < \nu_0$ seems to be satisfied. These $NbSe_3$ data show significant motional narrowing only for $E/E_T > 3$ where $\nu_d =$ 15 MHz while the hyperfine width is about $\nu_1 = 30$ kHz. ν_d is somewhat larger than $\nu_0 = 10$ MHz. However Ross [35] mentions that the noise spectra recorded in the range $E/E_T \leqslant 3$ lead to anomalously high values of ν_n/j : this is a strong indication that the CDW is moving only in a small part of the sample.

In blue bronze ν_0 is activated [36] and to satisfy the condition $\nu_0 < \nu_d < \nu_1$, as discussed by Tucker *et al.* [34], the temperature must be raised above $T = 65$ K and the electric field must be kept sufficiently low, $E/E_T \leqslant 3$. The data of figure 10 show that for $T \geqslant 69$ K and E/E_T between 2.3 and 3 the static fraction is about $f_s = 20$ %. These data do not rule out the model of Tucker *et al.* [34] for $E/E_T < 2$ but certainly do not support it for larger values. The current is inhomogeneous in the sample and a fraction of 20 % in which the CDW remains static is reasonable and explains the data without sudden jumps by 2 π of the phase. Our earlier measurement [4] on sample $\neq 1$ gave a static fraction of 40 % at 78 K and $E/E_T \approx 3$ showing that this value depends on sample and electrode contact quality.

The question of whether one can avoid a large static fraction of CDW in the sample close to the threshold field ($E/E_T < 3$) is still open. Nevertheless, our results indicates that the

motional narrowing is not dependent on the ratio ν_0/ν_d as suggested by Tucker *et al.* [34]. On the contrary, they suggest that the static fraction is *decreased* at high temperature by thermal depinning.

7.3 COHERENCE AND TEMPORAL FLUCTUATIONS OF THE MOTION OF THE CDW. — In absence of temporal fluctuations and instabilities of the CDW velocity the correlation function of the transverse magnetization $G(t)$ and the variation of the spin-echo amplitude $S(\tau)$ would be periodic and only damped by the usual spin-spin interaction. This dipolar spin-spin relaxation rate T_{2d} was found to be equal to 4.8 ms. We attribute any shortening of this damping constant to fluctuations in the temporal variation of the phase which introduce a loss of memory in the time-dependence of the local nuclear frequency (see Sect. 5.4).

First let us discuss the field dependence of the spin-spin relaxation rate at relatively high temperature. Such measurements were performed at 63 K and 77 K with differing results. A superposition of a motionally narrowed line on to a static spectrum is observed ; the intensity of the latter decreases with field and temperature. The spin-spin relaxation may be described by two time-constants corresponding to the dynamic (T_{2F}) and the static part (T_{2d} = 4.8 ms) of the line.

At 63 K a clear distinction between a static and a fast decaying dynamic component can be made. The relaxation rate is only weakly dependent on the field. If the model of section 5.4 with rare and large phase fluctuations is assumed then the product $n = T_{2F}\,\nu_d$ corresponds to the number of coherent oscillations. ($T_{2F} = \Gamma^{-1}$). At the lower field ($E/E_T \approx 3$) we find $\nu_d = 25$ kHz, $T_{2F} = 1$ ms and $n \approx 25$. Thus the CDW remains coherent for about 25 oscillations at any given nucleus.

Contrary to the 63 K measurement, the relaxation at 77 K was found to be strongly dependent on E/E_T, T_{2F} decreases sharply with decreasing field. This may reflect that the motion is more chaotic for fields near threshold than for large ν_d. It is related to the problem of how large is the part of the sample in which the CDW is really static for small fields. As the field approaches E_T from above the ν/j ratio increases showing that the fraction in which a CDW current with a steady component flows decreases. On the other hand both the lineshape analysis and the relaxation shows that in most of the sample the CDW remains fluctuating at high temperatures and low fields. Thus we believe there are regions of the sample for which the average CDW current is zero ($\bar{\dot{\varphi}}(t) = 0$) but where large amplitude fluctuations occur, fast enough to narrow the NMR line and increase the relaxation rate.

The fast decaying component of the relaxation at high temperature and low value of E/E_T is non-exponential, Gaussian like, characteristic of a spatial distribution of Γ. This is related to the inhomogeneity of the current distribution. At regions where the field is just sufficient to depin the CDW but no steady current flows the phase fluctuations have a large amplitude and are random while in regions where a steady current flows the phase changes with a constant rate and fluctuations are less important.

In high fields and low temperatures the sidebands and oscillations of the spin-echo amplitude give ample evidence for a coherent motion. A shortening of the spin-spin relaxation rate due to phase fluctuations is however still observed. The random phase fluctuations give rise to a relaxation rate $\Gamma = T_{2F}^{-1} = (T_2')^{-1} - (T_{2S})^{-1}$ where T_2' and T_{2S} are the measured relaxations rates under and without current. T_2' is measured by spin-echo delay times for which the oscillation due to coherentness is sufficiently damped. Applying the model of large amplitude fluctuations we find at 43 K (47 K) $\Gamma^{-1} = 15 \times 10^{-3}$ s (6×10^{-3} s), $\nu_d = 1.7 \times 10^3\ s^{-1}$ ($7.5 \times 10^3\ s^{-1}$) and $n_c = 25(45)$.

The large amplitude fluctuations model is not justified, however, at fields much above threshold where the opposite limit of small amplitude fluctuations with a short correlation

time is more reasonable. For this we found (Sect. 5.4)

$$(T_{2F})^{-1} = (2\pi\nu_1)^2 \overline{\delta\varphi^2}\,\tau_c$$

from which $\overline{\delta\varphi^2}\,\tau_c = 6 \times 10^{-8}$ s and 1.6×10^{-7} s for 43 K and 47 K respectively.

From the relaxation rate T_{2S} the intrinsic linewidth of the voltage noise oscillations $P(\nu)$ may be estimated. This width decreases with temperature, at about 50 K from T_{2F} we estimate a width of 100 Hz. This is much less than the inhomogeneous width observed by the noise frequency analyser, T_{2F} corresponds to the fluctuations of the phase winding rate at a fixed position.

Conclusions.

Joint transport, noise, and NMR measurements on the same single crystal — *in situ in the NMR coil* — have proved to be a very powerful way to investigate the dynamics of the sliding CDW. Beyond the evidence for the CDW motion as a bulk property — which comes out from the motional narrowing of the NMR spectrum — a number of points have been established in the blue bronze $Rb_{0.3}MoO_3$ which we think to be representative for the whole class of materials in which the CDW can be depinned by the application of an electric field.

The observation of sidebands in the NMR spectra as well as the oscillating behaviour of the spin-echo amplitude provide a direct measurement of the bulk winding rate of the phase ν_d. They provide a definite proof for a coherent modulation of the local hyperfine field at any given nucleus in the crystal, which in turn demonstrates that the sliding motion of the CDW is coherent within the time scale of the NMR experiment. Comparison with the noise spectra recorded at the same applied electric field and temperature establishes that the bulk winding rate of the phase ν_d is equal to the « noise » frequency ν_n with an accuracy better than 10 %. This rules out all theoretical models which predict a ratio ν_n/ν_d different from one [13, 14].

Experimental NMR spectra obtained at a fixed high value of the ratio E/E_T in the temperature range 40 to 60 K have been fitted to the theoretical lineshapes calculated under the assumption that the noise spectra correspond to the static spatial distribution of the CDW velocities in the crystal. The accuracy of the fit demonstrates the validity of this assumption ; it also allows to verify the long-assumed relationship $j = nev_{CDW}$ with an accuracy better than 10 %, thus establishing that *all the electrons condensed below the Peierls gap are involved in the Fröhlich mode.*

We have established a number of general features of the voltage noise spectrum. In the temperature range 40 to 60 K, the noise spectra obtained at high fixed values of E/E_T can be scaled on to each other despite three orders of magnitude variation of their mean frequency and the non linear conductivity. This indicates that the distribution of CDW velocities remains the same in this whole temperature range. Also the noise power $|V(t)|^2$ is roughly constant in the same temperature range, in spite of the variation of σ_{CDW}. This should be taken into account in any microscopic theory on the origin of the narrow band noise [12]. Another feature, following from the interpretation of the joint NMR and noise experiments, is that the low frequency tail observed in the noise spectra corresponds to a low frequency tail in the velocity distribution. This means that in some parts of the crystal, due to a stronger interaction with defects, the sliding motion of the CDW is very slow.

Our experiments can be fully interpreted by considering the crystal as a collection of independent domains within each of them an incommensurate CDW is sliding with a nearly uniform velocity. However, we cannot exclude that the « domains » are in fact separated by the paths of localized CDW defects, e.g. dislocation loops. Except for fields very close to the

threshold, nuclei far from the paths of dislocations will experience a relatively constant phase drift. For values of the electric field close to the threshold ($E/E_T < 3$) the CDW stays pinned in some parts of the crystal. This effect, which is proven by NMR experiments, is strongly dependent on the quality of the contacts and may lead to an anomalously high value of ν_n/j_{CDW}. As explained in section 7.2 we believe that this problem is not restricted to the blue bronzes, but is also present in $NbSe_3$ and is at the origin of the anomalous features of the NMR data in $NbSe_3$ [3a] reported by Ross *et al.* The temperature dependence of this static fraction is rather surprizing, it decreases with increasing temperature, leading to the unexpected conclusion that in some parts of the crystal, where there is no or negligible CDW current, the fluctuations of the phase are large enough to motionally narrow the NMR line.

Finally we have addressed the problem of the stochastic fluctuations of the CDW velocity within a time scale smaller than the NMR window, i.e. the spin-spin relaxation time. While the width of the sidebands of the NMR lineshape results from an inhomogeneous static distribution of velocities within the crystal, the width of the central line or more precisely the spin-spin relaxation rate as measured by spin-echo is affected by the stochastic temporal fluctuations of v_{CDW}. The correlation function of the transverse nuclear magnetization, which is periodic in the case of a periodic modulation of the local hyperfine field, becomes damped when stochastic fluctuations are present, $(T_2)^{-1}$ measures the strength of this damping. Our experiments have shown that $(T_2)^{-1}$ is increasing with temperature ; above 60 K it decreases with increasing applied electric field. Using simple approximations to relate $(T_2)^{-1}$ to the correlation time and the amplitude of the fluctuations of the CDW velocity we conclude that the average number of coherent oscillations at a nucleus in the crystal is of the order of 25-50.

A number of problems are left open which would deserve new experiments : e.g. the dynamics of the CDW when the applied electric field is in the vicinity of the threshold is poorly understood yet, especially when the thermal fluctuations becomes important. A clear separation between the CDW intrinsic bulk behaviour and artifacts induced by the quality of the electrical contacts will require a very careful study. But the most obvious extension of this work will be the study of the undamped sliding CDW regime recently observed at very low temperature [37].

References

[1] For a review, see : a) Charge Density Waves in Solids, Eds. G. Hutiray and J. Solyom, *Lect. Notes Phys.* **217** (Springer Verlag, New York) 1985 ; b) Proceedings of the XV Yamada Conference, *Physica* **143B** (1986).

[2] ONG N. P. and MONCEAU P., *Phys. Rev.* **B 16** (1977) 3367.

[3] a) ROSS J. H., WANG Jr. Z. and SLICHTER C. P., *Phys. Rev. Lett.* **56** (1986) 663 ;
b) SÉGRANSAN P., JANOSSY A., BERTHIER C., MARCUS J. and BUTAUD P., *Phys. Rev. Lett.* **56** (1986) 1854 ; in reference [1b], p. 120 ;
c) NAMURA K., KUME K. and SATO M., *J. Phys.* **C 19** (1986) L289.

[4] JANOSSY A., BERTHIER C., SÉGRANSAN P. and BUTAUD P., *Phys. Rev. Lett.* **59** (1987) 2348.

[5] FLEMING R. and GRIMES C. C., *Phys. Rev. Lett.* **42** (1979) 1423.

[6] BERTHIER C. and SÉGRANSAN P., Low Dimensional Conductors and Superconductors, *NATO Advanced Science Institutes Series B Physics* **155**, Eds. D. Jérome and L. C. Caron (Plenum Press NY) 1987, p. 455.

[7] BUTAUD P., SÉGRANSAN P., BERTHIER C. and JANOSSY A., to be published.

[8] FUKUYAMA H. and LEE P. A., *Phys. Rev.* **B 17** (1978) 535.

[9] LEE P. A. and RICE T. M., *Phys. Rev.* **B 19** (1979) 3970.

[10] FLEMING R. M., DUNN R. G. and SCHNEEMEYER L. F., *Phys. Rev.* **B 31** (1985) 4099.
[11] This was suggested by MEZEI F. and ZAWADOWSKY A.
[12] ONG N. P., VERMA G. and MAKI K., *Phys. Rev. Lett.* **52** (1984) 663 ;
ONG N. P. and MAKI K., *Phys. Rev.* **B 32** (1985) 6582.
[13] BARDEEN J., *Phys. Rev. Lett.* **55** (1985) 1010.
[14] MONCEAU P. *et al.*, *Phys. Rev.* **B 25** (1982) 931.
[15] We are grateful to MARCUS J. (L.E.P.E.S., C.N.R.S. Grenoble) for having grown the single crystals used in this work.
[16] GRAHAM J. and DE WADSLEY H., *Acta Crist.* **20** (1966) 93.
[17] GORKOV L. P., DOLGOV E. N., *Zh. Eksp. Teor. Fiz.* **77** (1979) 396 ;
FORRO L., COOPER J. R., JANOSSY A. and KAMARAS K., *Phys. Rev.* **B 34** (1986) 9047.
[18] DOUGLASS D. C., SCHNEEMEYER L. F. and SPENGLER S. E., *Phys. Rev.* **B 36** (1987) 1831.
[19] BAUGHER J. F., TAYLOR P. C., OJA T. and BRAY P. J., *J. Chem. Phys.* **50** (1969) 4919.
[20] DAS T. P. and HAHN E. L., *Solid State Phys. Suppl. I,* Eds. F. Seitz and D. T. Turnbull (Academic Press, New York) 1958.
[21] WEINBERGER B. R., *Phys. Rev.* **B 17** (1978) 566.
[22] SCHUTTLE W. J. and DE BOER, *Acta Cryst. B*, to be published.
[23] POUGET, J. P., KAGOSHIMA S., SCHLENKER C. and MARCUS J., *J. Phys. Lett. France* **44** (1983) L113.
[24] BLINC R., *Phys. Rep.* **79** (1981) 331 ;
BLINC R., PRELOVSEK P., RUTAR V., SELIGER J. and ZUMER S., in Incommensurate Phases in Dielectrics, Eds. R. Blinc and A. P. Levanyuk (Elsevier Science Publishers, BV) 1986, Ch. 4.
[25] MCMILLAN W. L., *Phys. Rev.* **B 12** (1975) 1187 ; *Phys. Rev.* **B 14** (1976) 1496.
[26] SATO M., FUJISHITA H. and HOSHINO S., *J. Phys.* **C 16** (1983) L877 ;
POUGET J. P., ESCRIBE-FILIPPINI C., HENNION B., CURRAT R., MOUDDEN A. H., MORET R., MARCUS J. and SCHLENKER C., *Mol. Liq. Cryst.* **121** (1985) 111.
[27] FLEMMING R. M., SCHNEEMEYER L. F. and MONCTON D. E., *Phys. Rev.* **B 31** (1985) 899.
[28] BUTAUD P., Thesis, Grenoble (1987).
[29] NOMURA K., KUME K. and SATO M., *Solid State Commun.* **57** (1986) 611.
[30] JANOSSY A., DUNIFER G. L. and PAYSON J. S., *Phys. Rev.* **B 38** (1988) 1577.
[31] KOGOJ M., ZUMER S. and BLINC R., *J. Phys. C Solid State Phys.* **17** (1984) 2415.
[32] ABRAGAM A., Principles of Nuclear Magnetism (Clarendon Press Oxford) 1961.
[33] DOUGLASS D. C., SCHNEEMEYER L. F. and SPENGLER S. E., *Phys. Rev.* **B 32** (1985) 1813.
[34] TUCKER J. R., *Phys. Rev. Lett.* **60** (1988) 1574 ;
TUCKER J. R., LYONS W. G. and GAMMIE G., *Phys. Rev.* **B 38** (1988) 1148.
[35] ROSS J. H., Thesis, University of Illinois (1986).
[36] CAVA R. J., FLEMMING R. M., LITTLEWOOD P., RIETMAN E. A., SCHNEEMEYER L. F. and DUNN R. G., *Phys. Rev.* **B 30** (1984) 3228.
[37] MIHALY G. and BEAUCHÊNE P., *Solid State Commun.* **63** (1987) 911.